Electrical Properties of $(Ba,Sr)TiO_3$ Thin Films Deposited on RuO_2 Electrode

Chi-Sun Park*
Department of Eletronic Engineering, Hanseo University, Seosan 352-820, Korea

In-Ki Kim
Department of Materials Science & Engineering, Hanseo University, Seosan 352-820, Korea

E-mail : Pcs98@hanseo.ac.kr

(Received 4 November 2000, Accepted 22 December 2000)

The variation of electrical properties of $(Ba,Sr)TiO_3$ [BST] thin films deposited on RuO_2 electrode with (Ba+Sr)/Ti ratio was investigated. BST thin films with various (Ba+Sr)/Ti ratio were deposited on RuO_2/Si substrates using *in-situ* RF magnetron sputtering. It was found that the electrical properties of BST films depends on the composition in the film. The dielectric constant of the BST films is about 190 at the (Ba+Sr)/Ti ratio of 1.0, 1.025 and does not change markedly. But, the dielectric constant degraded to 145 as the (Ba+Sr)/Ti ratio increase to 1.10. In particular, the leakage current mechanism of the films shows the strong dependence on the (Ba+Sr)/Ti ratio in the films. At the ratio of (Ba+Sr)/Ti=1.025, the Al/BST/RuO_2 capacitor show the most asymmetric behavior in the leakage current density vs. electric field plot. It is considered that the leakage current of the (Ba+Sr)/Ti=1.025 thin films is controlled by the barrier-limited process, i.e. Schottky emission.

Keywords : BST, DRAM, Capacitor, Dielectirc

1. INTRODUCTION

$(Ba,Sr)TiO_3$ [BST] is an attractive capacitor material for dynamic random access memory (DRAM) with 1 Gbit or higher density and is expected to replace the conventional SiO_2 or Ta_2O_5 dielectrics because of its high dielectric constant and relatively low leakage current.[1] It is difficult to obtain the required charge storage capacitance for DRAM over 1 Gbit using SiO_2 or Ta_2O_5 dielectrics because extremely complex fabrication processes to produce stack or trench structures are necessary. [2] $(Ba,Sr)TiO_3$ has a much higher dielectric constant than the conventional SiO_2 and Ta_2O_5 dielectrics. The electrical properties of BST thin films can be easily controlled in the paraelectric phase by controlling the Ba/Sr ratio. Therefore, it is possible to eliminate the problem of fatigue caused by ferroelectric domain switching, as observed in $Pb(Zr,Ti)O_3$. [3]

Because of a higher substrate temperature and an oxidizing atmosphere necessary for the deposition of high dielectric BST thin films, refractory noble metal , such as Pt and Pd, have been used as the bottom electrodes in the high dielectric thin film capacitors.[4~6) However, these noble metal are not suitable for precise submicron patterning for VLSI application. Furthermore, Takemura et al.[7] reported that the barrier ability of Pt against oxygen was not sufficient. Also, another major problem with Pt bottom electrode is the formation of hillocks at higher temperature.[8] RuO_2 is a representative rutile-type conductive metal oxide to overcome above mentioned problems for application in VLSI electrode and shows good stability at elevated temperature.[9,10] RuO_2 thin films has been an attractive material for interconnects, contacts, gate electrode, and diffusion barriers in Si devices, because it has relatively low resistivity and acts as a diffusion barrier against oxygen. [11~12] Pan and Desu [13] reported the reactive ion etching of RuO_2 thin films with gas mixture of O_2/CF_3CFH_2. However, there are few studies on the application of RuO_2 thin films as the bottom electrode of the high dielectric BST thin films for DRAM capacitor. Also, the electrical properties of the BST thin films on RuO_2 electrode has not been studied extensively. In this study, the electrical properties of high dielectric BST thin films deposited on RuO_2 bottom electrode was investigated with various (Ba+Sr)/Ti ratio in the films.

Especially, the variation of the leakage current mechanism in the BST thin films on RuO_2 electrode was investigated with the (Ba+Sr)/Ti ratio in the films.

2. EXPERIMENTAL

As a bottom electrode, the 100 nm thick RuO_2 thin film was deposited on p-Si(100) substrate by RF magnetron sputtering with compressed RuO_2 powder target. The O_2/Ar ratio in the plasma gas was maintained in 1/9 which shows most planar surface morphology in our previous studies. RuO_2/Si substrate for the deposition of BST thin film was prepared. A $(Ba,Sr)TiO_3$ target with (Ba+Sr)/Ti=1.0, 1.025, 1.05, 1.10 was prepared by mixing 99.98% $BaTiO_3$, 99.9% $SrTiO_3$ powders with excess 99.5% BaO, SrO powders. The in-situ deposition conditions of BST thin films are summarized in Table I. In order to carry out the electrical measurements, Al upper electrodes with a radius of 100 μm, patterned using a stainless steel shadow mask, were fabricated on the BST thin films by thermal evaporation.

The phase and crystallinity of the $(Ba,Sr)TiO_3$ thin films were determined by X-ray diffraction (XRD) with Cu K_α radiation, using Rigaku RAD-C system (40kV,40mA). The morphology of the thin films was investigated using a scanning electron microscope (SEM). The Rutherford Backscattering Spectrometry (RBS) and the Auger Electron Spectroscopy (AES) methods were used to investigate the composition in BST thin films and the interface between BST thin films and RuO_2 bottom electrode. The leakage current characteristics were measured using an HP4145B semiconductor parameter analyzer. The dielectric constants were measured using an HP4280A 1MHz C meter/CV plotter.

Table 1. Deposition conditions of $(Ba,Sr)TiO_3$

Substrate temperature	550 ℃
Sputtering gas	O_2/Ar =5/5
Deposition pressure	10 mTorr
Target size	3 inch
RF power	130 W
(Ba+Sr)/Ti in target	1.0, 1.025, 1.05, 1.10

3. RESULTS AND DISCUSSION

Fig. 1 shows the surface morphology and the cross-sectional view of 150 nm thick BST thin films deposited on RuO_2 bottom electrode with various (Ba+Sr)/Ti ratios in the films. It is confirmed that the BST thin films deposited on columnar RuO_2 thin films also show the columnar grain as the same way in RuO_2 electrode. Furthermore, no marked interdiffusion between BST and RuO_2 was observed and stable interface was maintained. The surface morphology of BST thin films is confirmed to be relatively planar for all specimen with various (Ba+Sr)/Ti ratios without remarkable changes in surface morphology.

However, as the (Ba+Sr)/Ti ratio changes in the films, the surface morphology shows some dependence on the composition. When (Ba+Sr)/Ti in the target is 1.0, it is observed that the surface morphology of the film is composed with faceted columnar grains which appear in the thin films with good crystallinity. In this case, the overall surface roughness is relatively higher than (Ba+Sr)/Ti = 1.025 BST thin films. Meanwhile, as the (Ba+Sr)/Ti ratio increases to 1.025, the surface roughness decreases as the result of the finer columnar grains in the films. As confirmed by composition analysis of BST thin films by AES and RBS, it is possible to assume that the stoichiometric BST thin films deposited with sputtering target of (Ba+Sr)/Ti =1.025 is most probable to form the BST thin films with ideal Perovskite structure. Furthermore , as the (Ba+Sr)/Ti ratios increase to 1.05 and 1.10, the columnar grains of BST thin films show more faceted morphology. The RuO_2 thin films, typical conductive oxide, are difficult to obtain planar surface morphology in the process of crystal growth because RuO_2 with relatively higher surface energy than Ru metal have

Transactions on Electrical and Electronic Materials, Vol.1, No.4 December 2000

tendency to grow in faceted structure. So, the roughness

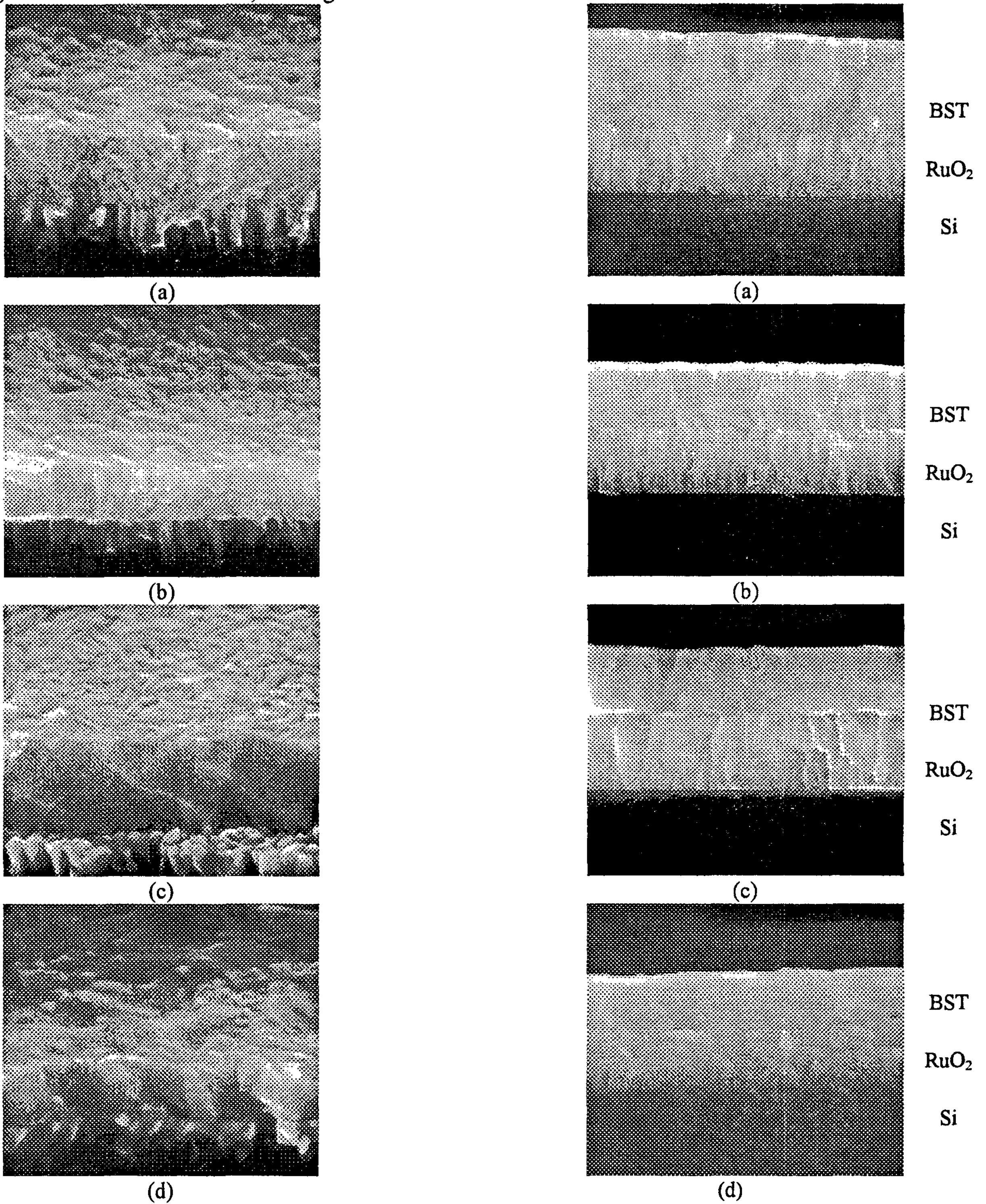

Fig. 1. Planar view and cross-sectional view of 150 nm BST on RuO_2 electrode with target of (a) (Ba+Sr)/Ti = 1.0 , (b) 1.025 , (c) 1.05 , (d) 1.10.

of BST thin films deposited on RuO_2 electrode with above characteristics are closely related with the surface roughness of bottom electrode.

As the surface morphology of BST thin films are affected by RuO_2 thin films with faceted structure, excess Ba and Sr in the films act as the strain source in the Perovskite structure. In order to release the stress in the lattice caused by excess Ba and Sr in the films, the lattice in Perovskite structure should arrange in the preferred orientation to lower the overall surface energy. These assumption is correlated with the change of preferred orientation in XRD patterns of BST thin films on RuO_2 with various (Ba+Sr)/Ti ratios. These various surface morphology with (Ba+Sr)/Ti ratio can affect the electrical characteristics of BST thin films. As the surface roughness of the films is larger, it is difficult to obtain uniform properties and the degradation of electrical properties is caused by localized high electric field because of the non-uniformity of the film thickness. These tendency could be discussed later in terms of electrical characteristics.

The phase formation and crystallinity of BST thin films with various (Ba+Sr)/Ti ratio was investigated by XRD analysis, as shown in Fig. 2. As confirmed by each XRD patterns, the phase formation of Perovskite BST is extensive for all compositions. However, for (Ba+Sr)/Ti ratio is 1.0 and 1.025, the preferred orientations of BST(111) peaks are confirmed in the patterns. In the case of (Ba+Sr)/Ti =1.05 and 1.10, the BST(110) peaks in the patterns are most intensive and show the preferred orientation. It is considered that the excess Ba and Sr existing in the BST lattice act as strain

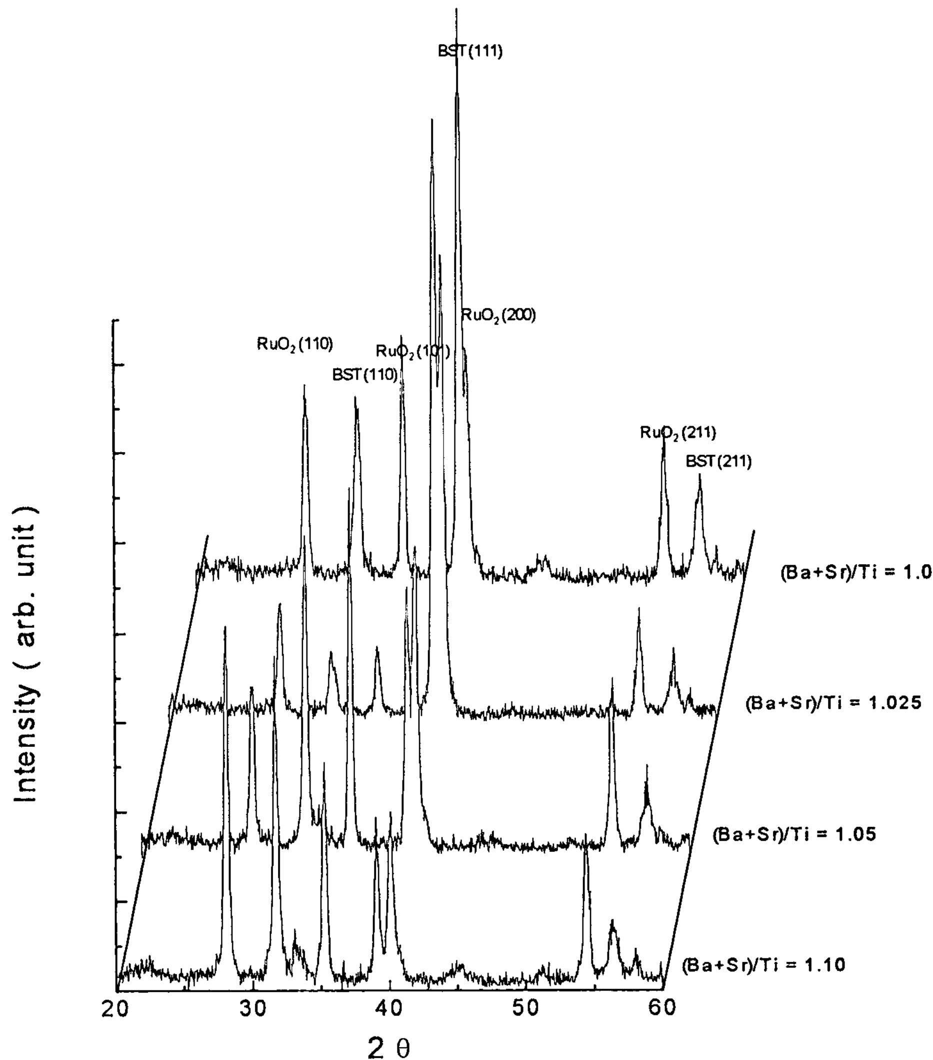

Fig. 2. XRD patterns from BST on RuO_2.

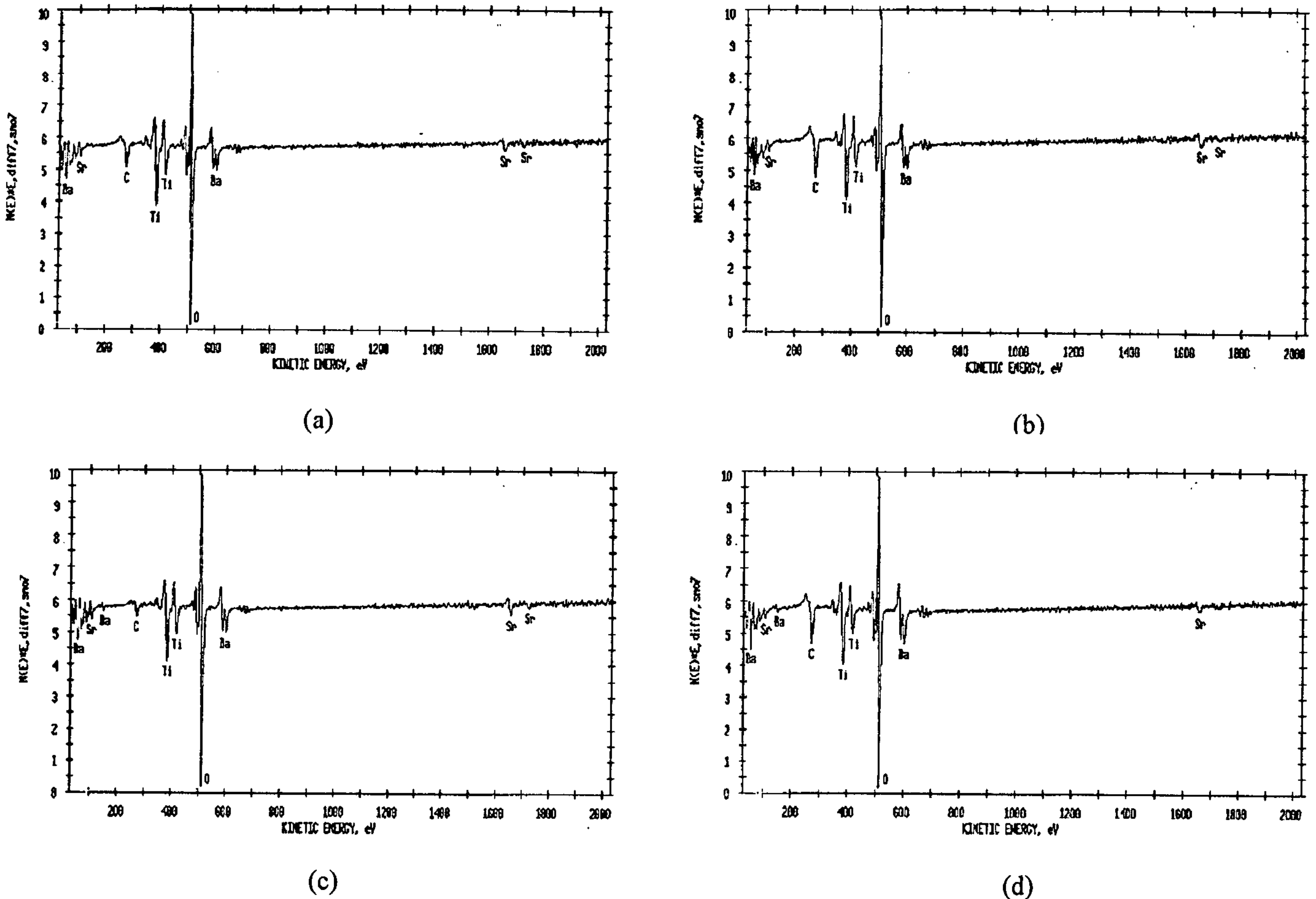

Fig. 3. AES surface spectrum of BST(150nm)/RuO_2(100nm) deposited with target of (a) (Ba+Sr)/Ti = 1.0, (b) (Ba+Sr)/Ti = 1.025, (c) (Ba+Sr)/Ti = 1.05, (d) (Ba+Sr)/Ti = 1.10.

(Ba+Sr)/Ti ratio in the sputtering target was 1.025, the deposited thin films approached the most stoichiometric composition. For (Ba+Sr)/Ti =1.025 sputtering target, the Ba:Sr:Ti:O ratio in the film is 0.45:0.55:1:3 which slightly deviate from stoichiometric composition of 0.5:0.5:1:3. Meanwhile, for the sputtering target of (Ba+Sr)/Ti=1.10, the Ba:Sr:Ti:O in the deposited film is 0.6:0.4:1:3 which deviate extensively from the stoichiometric composition. In this case, the proportion of Ba is larger than that of Sr. It is difficult to maintain the paraelectric properties for this case.

The distribution of each elements and the composition in the films were investigated by Auger Electron Spectroscopy(AES), as shown in Fig. 3. AES surface spectrum confirm that the surface of BST thin film is composed with only Ba, Sr, Ti and O including C. Also, no Ru metal element from RuO_2 bottom electrode was detected in the AES surface spectrum. It means no remarkable inter-diffusion between BST thin films and RuO_2 bottom electrode. This consideration can be confirmed by the AES depth profile. As confirmed by AES depth profile, each elements distribute uniformly without the abrupt changes in composition.

This deficiency of oxygen at the interface between BST and RuO_2 could act as the control factor of the lectrical properties of Al/BST/RuO_2 capacitor. The expansion of the oxygen deficient range observed near BST/RuO_2 interface as the increase of (Ba+Sr)/ti is considered to be caused by the increase of reaction of excess Ba and Sr with oxygen in the RuO_2 bottom electrode. The concentration of oxygen decreases at the BST/RuO_2 interface and show the discontinuous distribution of the oxygen element. This could affect the electrical properties of BST/RuO_2 capacitor which is controlled by the interface state. This oxygen deficiency is considered to occur at the initial step of BST thin films depostion.

Fig. 4 shows the relation between applied voltage and dielectric constant with the various (Ba+Sr)/Ti ratio in the films. As observed in Fig. 5, the relation shows

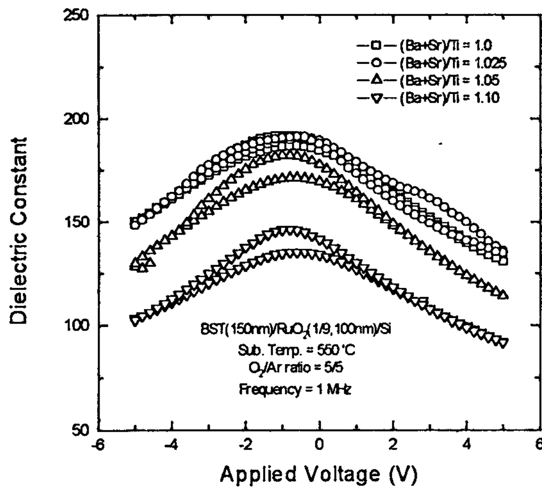

Fig. 4. Dielectric constant vs. Applied voltage plot of BST/RuO_2 with various (Ba+Sr)/Ti ratio.

typical dielectric characteristics. The dielectric constant of BST thin films with (Ba+Sr)/Ti =1.0 and 1.025 shows almost same values overall applied voltage. Meanwhile, as the (Ba+Sr)/Ti ratio increases to 1.05 and 1.10, the overall dielectric constant decrease

The composition in the deposited BST thin film shows the most stoichiometric composition when the (Ba+Sr)/Ti ratio in the sputtering target is 1.025. Over (Ba+Sr)/Ti=1.025, the excess Ba and Sr in the perovskite BST lattice is considered to decrease the overall dielectric constant. The dielectric constant calculated from maximum capacitance is 190 for (Ba+Sr)/Ti=1.0 and 1.025 and 145 for (Ba+Sr)/Ti=1.10, as shown in Fig. 4. Furthermore, the reliability of BST thin films deposited on RuO_2 is tested by the variation of dielectric constant with applied frequency (Fig. 5). The dielectric constant of BST thin film with ta (Ba+Sr)/Ti = 1.025 is maintained high dielectric constant to higher applied frequency. The dielectric constant of BST thin films with (Ba+Sr)/Ti ratio over 1.025 decreases as the ratio increase and maintains to lower frequency.

The variation of BST thin films on RuO_2 bottom electrode with (Ba+Sr)/Ti ratio is shown in Fig. 6. It shows strong dependence of leakage current on the (Ba+Sr)/Ti ratio. The leakage current characteristics of BST thin films show the symmetric and asymmetric relation in Leakage current vs. Electrical field plot. These symmetric and asymmetric relation in the leakage current vs. Electric field will be explained later related with leakage current mechanism in BST thin films on RuO_2 bottom electrode. The leakage current density at +1.5V is shown in Fig. 6. The lowest leakage current density of BST thin films is $1x10^{-6}$ A/cm^2 for (Ba+Sr)/Ti=1.025. Meanwhile, as the (Ba+Sr)/Ti ratio increases, the leakage current density increases. This result will be confirmed later in the consideration of leakage current mechanism.

Fig. 7 shows the Leakage current vs. Electrical field

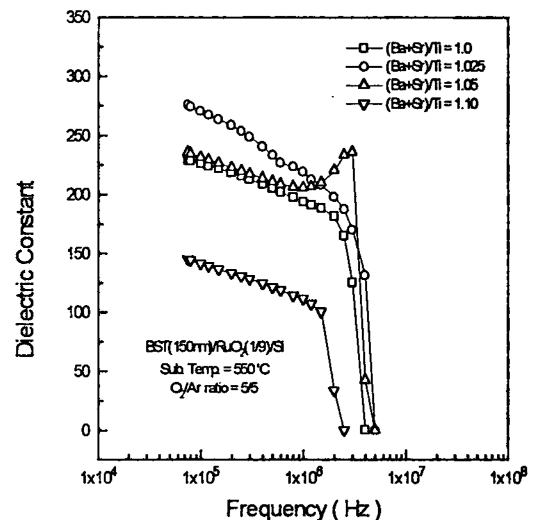

Fig. 5. Dielectric consnt vs. Frequency plot of BST/ various (Ba+Sr)/Ti ratio.

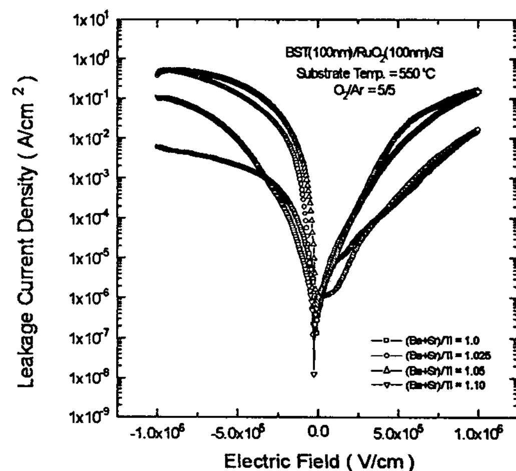

Fig. 6. Leakage current of BST/RuO_2 with various (Ba+Sr)/Ti ratio Leakage current vs. Electrical field plot of BST/RuO_2.

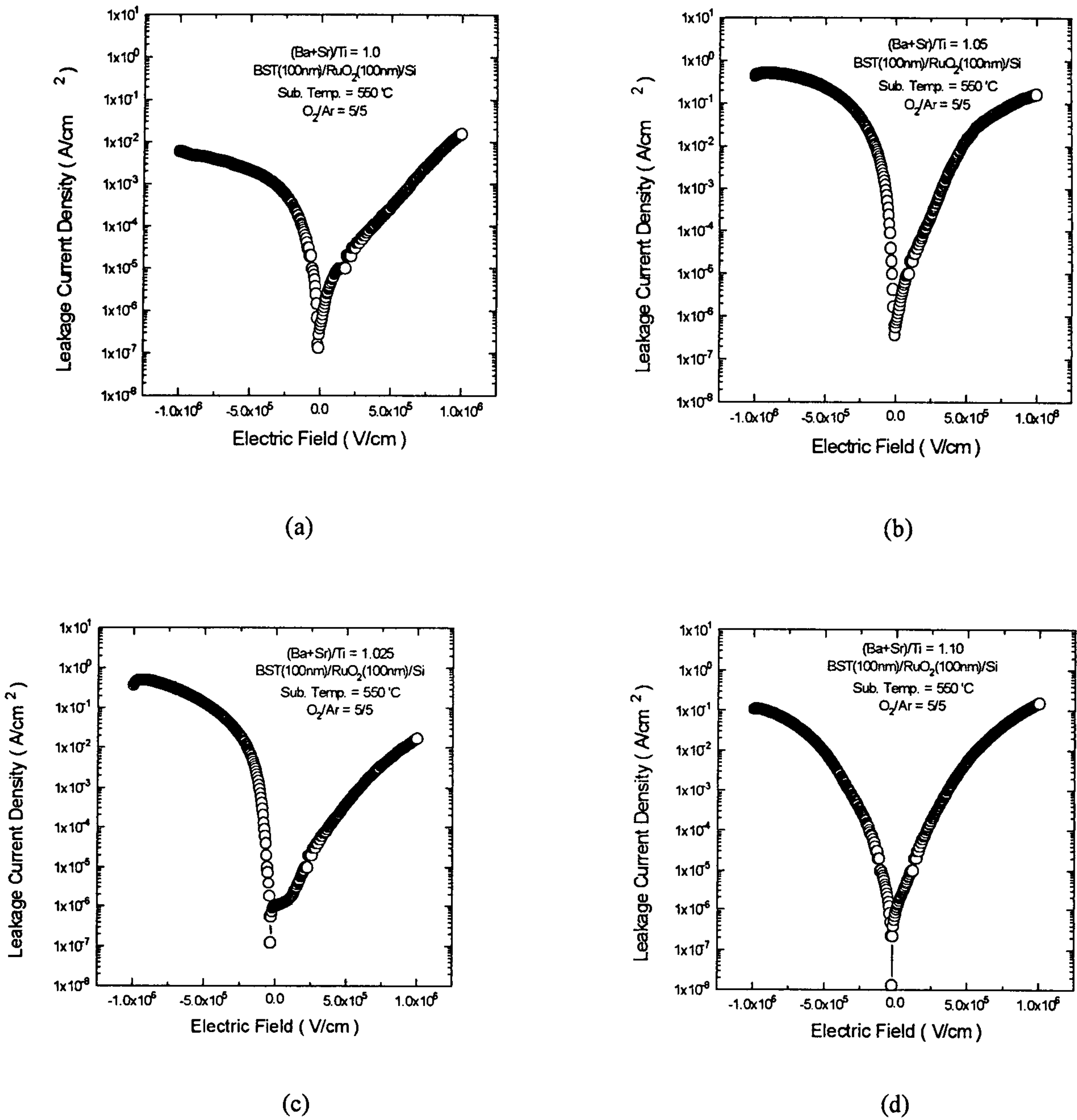

Fig. 7. Leakage current vs. Electric field plot of BST/RuO_2 with (Ba+Sr)/Ti = (a) 1.0, (b) 1.025, (c) 1.05, (d) 1.10.

plot to confirm the variation in the symmetric and asymmetric characteristics. For (Ba+Sr)/Ti=1.0, the leakage current shows symmetric characteristics with electric filed. Meanwhile, as the (Ba+Sr)/Ti ratio increases to 1.025, the leakage current density measured at -1MV/cm is 100 times larger than that at +1MV/cm to deviate markedly from the symmetry. It is assumed that this asymmetry in the leakage current is controlled by barrier-limited conduction mechanism caused by the potential barrier at BST/RuO_2 interface. As the (Ba+Sr)/Ti ratio increases over 1.025, the relation between leakage current and electric field approaches to symmetric characteristics. It is considered to be caused by the defects in the films induced by excess Ba and Sr as the (Ba+Sr)/Ti ratio increases. These defects in the films act as transition level in the energy band and supply the easy path to electron conduction by trapping and detrapping process independent of the potential barrier at the BST/RuO_2 interface.

The variation of leakage current mechanism with (Ba+Sr)/Ti ratio is investigated by the relation between

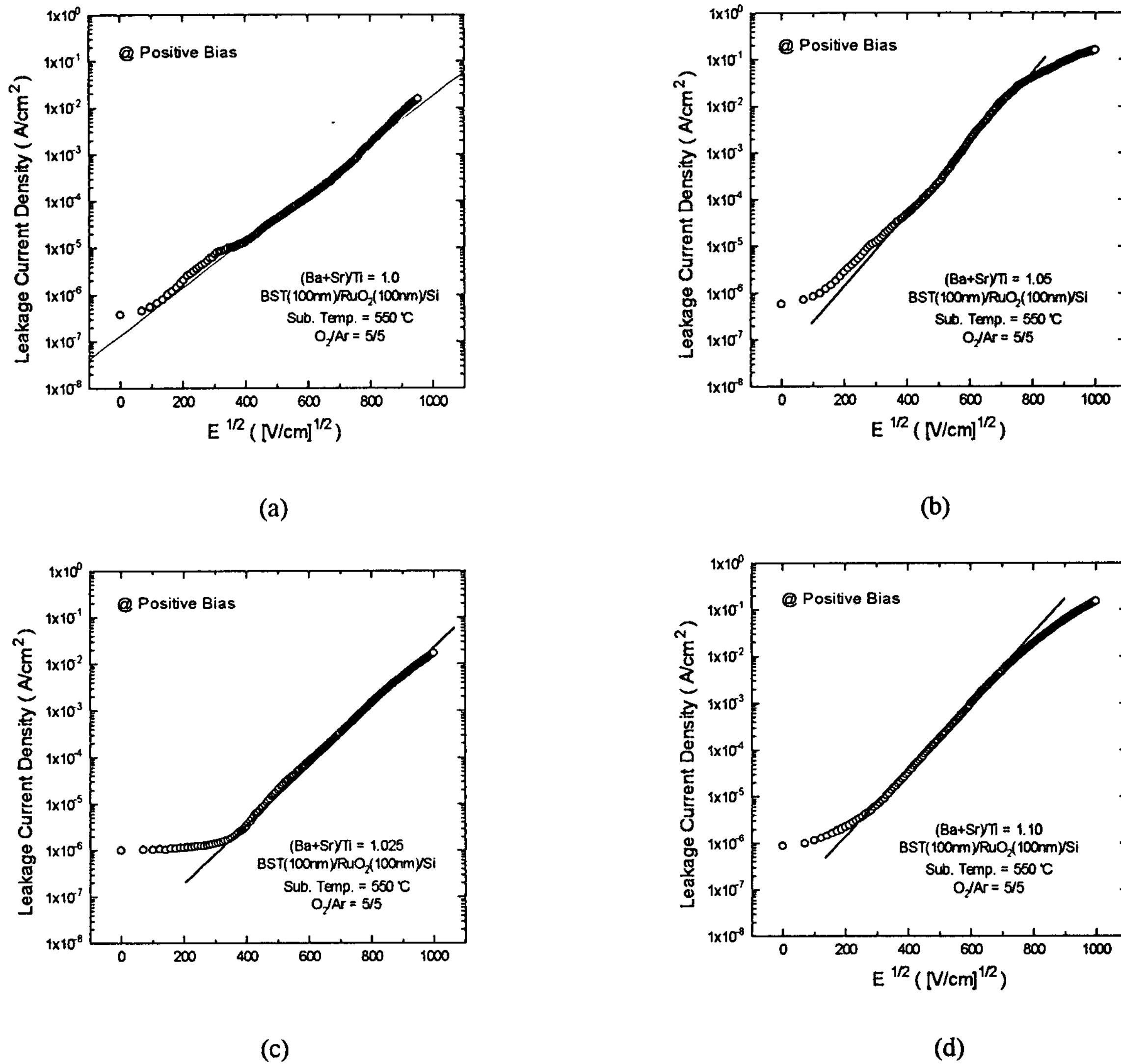

Fig. 8. Leakage current vs. Root Electric field plot of BST/RuO_2 with (Ba+Sr)/Ti = (a) 1.0, (b) 1.025,(c) 1.05, (d) 1.10.

the leakage current density and the square root electric field (Fig.8). For all (Ba+Sr)/Ti ratios, the leakage current density show the linear dependence on the square root electric field. So, the leakage current mechanism in the BST/RuO_2 capacitor is considered to be controlled by the bulk-limited Poole-Frenkel emission or the barrier-limited Schottky emission. In order to distinguish the difference in two leakage current mechanism, the symmetry and the asymmetry in the leakage current vs. electric field plot. For (Ba+Sr)/Ti=1.025, the leakage current vs. electric field plot shows the most asymmetric characteristics that the leakage current in the BST film is considered to be controlled by barrier-limited Schottky emission. For other compositions except for (Ba+Sr)/Ti=1.025, the plots show symmetric characteristics that the bulk-limited Poole-Frenkel emission is thought to be dominant leakage current mechanism in the BST thin films.

Potential barrier height of BST thin film with (Ba+Sr)/Ti=1.025 which shows the behavior of Schottky emission was calculated The variation of leakage current with temperature was investigated to calculate the potential barrier height from typical conduction equation of Schottky emission (Fig. 9).

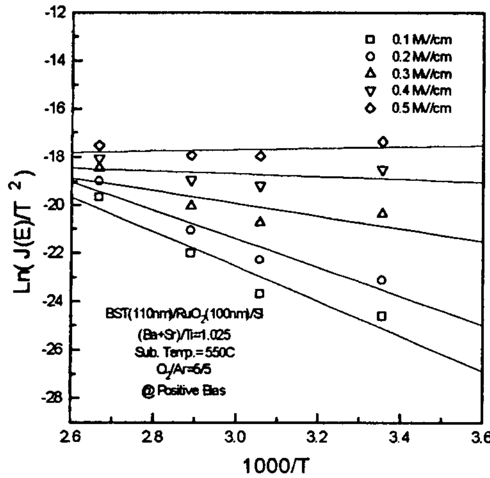

Fig. 9. Ln($J(E)/T^2$) vs. 1000/T plot with various elect BST on RuO_2 electrode with (Ba+Sr)/Ti = 1.025.

The potential barrier height at BST/RuO_2 interface calculated from Fig. 9 is 1.26eV, as shown in Fig. 10. In order to confirm this value, the barrier height vs. square root electric field plot was investigated(Fig. 11). It shows the linear relation between the barrier height and the square root electric field which coincides with the

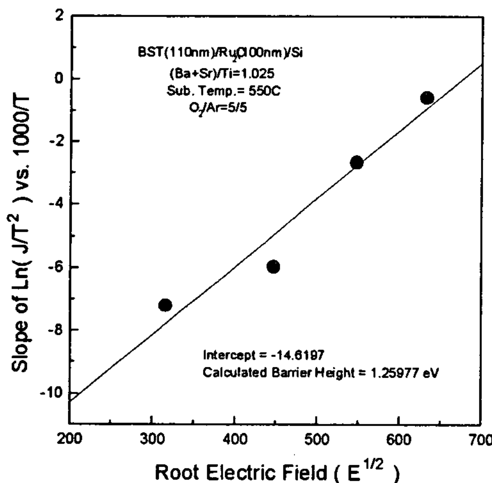

Fig. 10. Slope of (Ln($J(E)/T^2$) vs. 1000/T) vs. $E^{1/2}$ plot of BST on RuO_2 electrode with (Ba+Sr)/Ti = 1.025 for calculation of barrier height.

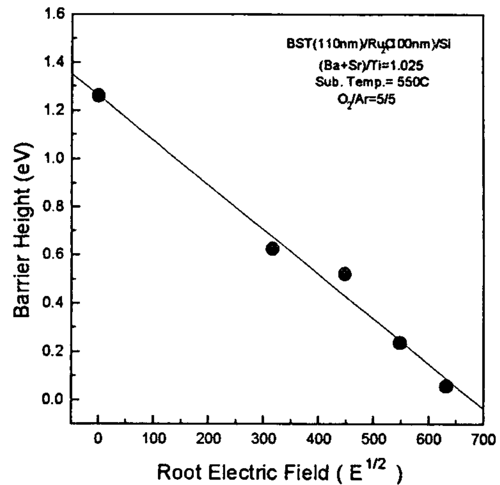

Fig. 11. Barrier height vs. $E^{1/2}$ plot of of BST on RuO_2 electrode with (Ba+Sr)/Ti = 1.025 for confirmation of barrier height.

linear relation as in the Schottky emission. BST thin films with (Ba+Sr)/Ti = 1.025 which shows the lowest leakage current density is thought to be controlled by the potential barrier at the BST/RuO_2 interface to lower the leakage current.

4. CONCLUSIONS

The BST thin films deposited on RuO_2 bottom electrode show the changes in the preferred orientation with (Ba+Sr)/Ti ratio in the films, but no extensive changes in the phase formation without the formation of second phase. However, the electrical properties of the films show strong dependence on the (Ba+Sr)/Ti ratio. The dielectric constants decrease as the (Ba+Sr)/Ti ratio increases while those of BST films with (Ba+Sr)/Ti = 1.0 and 1.025 show similar values. The leakage current in the BST thin film shows its lowest value when the (Ba+Sr)/Ti ratio is 1.025 because the film has the most stoichiometric composition to eliminate the defect-induced conduction. The leakage current mechanism for (Ba+Sr)/Ti = 1.025 shows the barrier-limited Schottky emission while in other compositions the leakage current is controlled by bulk-limited Poole-Frenkel emission.

REFERENCES

[1] A. Yuuki, M. Yamamuka, T. Makita, T. Horikawa, T. Shibano, N. Hirano, H. Maeda, N. Mikami, K. Ono, H. Ogata and H. Abe, *Int. Electron Device Meet.*

Tech. Dig., p. 119, 1995.

[2] S. Yamamichi, K. Takemura, T. Sakuma, H. Watanabe, H. Ono, K. Tokashiki, E. Ikawa and Y. Miyasaka, Proc. *9th IEEE Int. Symp. Application of Ferroelectrics eds. R. K. Pandey, M. Liu and A. Safari, Pennsylvania, USA*, p. 74, 1994.

[3] T. Kawahara, M. Yamamuka, T. Makita, J. Naka, A. Yuuki, N. Mikami and K. Ono, *Jpn. J. Appl. Phys.*, Vol. 33, p.5129, 1994.

[4] Y. Miyasaka and S. Matsubara, *Proceedings of the 1990 IEEE 7th International Symposium on the Applications of Ferroelectrics(IEEE Service Center, Piscataway)*, p. 121, 1991.

[5] S. Yamamichi, T. Sakuma, T. Hase, and Y. Miyasaka, *in Ferroelectric Thin Films II, edited by A. I. Kingon, E. R. Myers, and B. Tuttle (Materials Research Society, Pittsburgh)*, Vol. 243, p.297, 1992.

[6] S. H. Paek, J. H. Won, K. S. Lee, J. S. Choi, C. S. Park, *will be published in Jpn. J. Appl. Phys.*, Vol. 35, Part 1, No. 11, 1996.

[7] K. Takemura, T. Sakuma, S. Matsubara, S. Yamamichi, H. Yamaguchi and Y. Miyasaka, *Proc. 4th Int. Symp. Integrated Ferroelectrics, Monterey*, p. 481, 1992.

[8] H. N. Al-Shareef, K. D. Gifford, P. D. Hren, S. H. Rou, O. Auciello and A. I. Kingon, *Proc. 4th Int. Symp. Integrated Ferroelectrics, Monterey*, p. 187, 1992.

[9] W. D. Ryden and A. W. Lawson, *Phys. Rev. B*, Vol. 1, p. 1494, 1970.

[10] R. G. Vadimsky, R. P. Frankenthal and D. E. Thompson, *J. Electrochem. Soc.*, Vol. 132, p. 2077, 1985.

[11] M. Wittmer, *J. Vac. Sci. Technol. A*, Vol. 2, p. 273, 1984.

[12] L. Krusin-Elbaum, M. Wittmer, and D. S. Yee, *Appl. Phys. Lett.*, Vol. 50, p. 1879, 1987.

[13] Wei Pan and Seshu B. Desu, *J. Vac. Sci. Technol., B*, Vol. 12, No. 6, p. 3208, 1994.